THE JOURNAL OF BIOLOGICAL CHEMISTRY VOL. 287, NO. 17, pp. 13532–13540, April 20, 2012

Structure-Function Relationships in [FeFe]-Hydrogenase Active Site Maturation*

Published, JBC Papers in Press, March 2, 2012, DOI 10.1074/jbc.R111.310797

Yvain Nicolet and Juan C. Fontecilla-Camps[1]

From the Metalloproteins Unit, Institut de Biologie Structurale "Jean-Pierre Ebel," Commissariat à l'Energie Atomique, CNRS, Université Joseph Fourier, 38027 Grenoble Cedex 1, France

Since the discovery that, despite the active site complexity, only three gene products suffice to obtain active recombinant [FeFe]-hydrogenase, significant light has been shed on this process. Both the source of the CO and CN^- ligands to iron and the assembly site of the catalytic subcluster are known, and an apo structure of HydF has been published recently. However, the nature of the substrate(s) for the synthesis of the bridging dithiolate ligand to the subcluster remains to be established. From both spectroscopy and model chemistry, it is predicted that an amine function in this ligand plays a central role in catalysis, acting as a base in the heterolytic cleavage of hydrogen.

Many metalloenzymes have complex active sites that require a series of proteins involved in the synthesis, transport, and insertion of their components and their subsequent maturation. Classic examples are nitrogenase (1), involved in nitrogen fixation, and the [NiFe]-hydrogenase, capable of oxidizing hydrogen and reducing protons depending on the physiological conditions and cellular location (Reactions 1 and 2) (2).

$$H_2 \leftrightarrow H^- + H^+$$
Reaction 1

$$H^- \leftrightarrow H^+ + 2e^-$$
Reaction 2

In both cases, there are >15 proteins involved in the assembly of the active site and the generation of functional protein. This minireview concerns the other "full-fledged" hydrogen-metabolizing enzyme, the [FeFe]-hydrogenase (2). (The [Fe]-hydrogenase from methanogens catalyzes only the first half-reaction (Reaction 1) (3).) Crystallographic studies have shown that its active site, called the H-cluster, contains three unusual types of iron ligands: CO, CN^-, and a small dithiolate [Fe_2]-bridging molecule, in addition to a regular [Fe_4S_4] subcluster (Fig. 1*A*) (4–6). It was then surprising to find that the *Chlamydomonas reinhardtii* [FeFe]-hydrogenase could be heterologously matured in *Escherichia coli*, which does not contain this enzyme, by coexpressing only two other algal gene products (HydE-F and HydG; HydE and HydF are coded by separate genes in other species) (7). This does not necessarily imply that they are sufficient, as other proteins from *E. coli* may substitute for those of *C. reinhardtii*. This is in fact suggested by the limited amounts of active [FeFe]-hydrogenase produced *in vitro* using purified maturases (8–10). What is clear, however, is that the substrate(s) for the synthesis of the active site ligands is present in *E. coli*. As will be shown below, the source for the synthesis of CO and CN^- has been elucidated (11–13), but the precursor(s) of the small dithiolate species remains to be identified. Because of this, the nature of its bridgehead atom has not been directly elucidated; however, as discussed below, indirect evidence and chemical inference strongly suggest that it is nitrogen.

[FeFe]-Hydrogenases are found in bacteria, unicellular algae, and protozoa, but they are absent in archaea. There is a general trend for bacterial enzymes to be significantly more active than protozoan enzymes. One intriguing observation that we discuss below is the presence of the structural gene for [FeFe]-hydrogenase and some hydrogenase activity in organisms that lack the three maturase genes.

Activity of [FeFe]-Hydrogenase Maturases

HydF: A Scaffold for the [Fe_2] Subcluster Assembly—Based on amino acid sequence analyses, HydF is constituted by a GTPase domain at the N-terminal region and a C-terminal domain containing three conserved cysteines, putatively responsible for the binding of an [FeS] cluster (7). Initial characterization of the HydF protein from *Thermotoga maritima* confirmed its GTPase activity, which is low compared with other enzymes in this class (14). In the same study, the authors confirmed that HydF reconstituted *in vitro* has an [Fe_4S_4] cluster bound by the three conserved cysteine residues. The fourth ligand of the cluster is exchangeable and is neither water nor nitrogen (14). Site-directed mutagenesis confirmed that both the GTP-binding site and the conserved cysteines are necessary for the activation of hydrogenase (15). Recently, Shepard *et al.* (16) demonstrated that the activity of the protein is GTP-specific and depends on the nature of the monovalent cation present in the buffer. Indeed, in the presence of K^+ instead of Na^+, HydF displays a higher activity, which is comparable with that of other GTPases. This activity is not dependent on the presence of the [Fe_4S_4] cluster. Subsequent studies using cell extracts demonstrated that the Hyd machinery is solely responsible for the assembly of the [Fe_2] subcluster (17). To be activated, hydrogenase requires the [Fe_4S_4] subcluster to be already bound at the active site. A general FeS biosynthetic machinery, such as the ISC system (18), most probably assembles this component of the H-cluster. Purified HydF, previously coexpressed with HydE and HydG, is capable of activating [Fe_4S_4]-containing hydrogenase (9). This shows that HydF is a scaffold protein that binds the products of HydE and HydG, assembles the [Fe_2] subcluster, and transfers it to hydrogenase. Both, homologously and heterologously overexpressed HydF proteins, coexpressed with HydG and HydE ($HydF^{EG}$) or expressed alone ($HydF^{\Delta EG}$),

* This work was supported by Agence Nationale de la Recherche Contract ANR-08-BLAN-0224-01 and by institutional funds from the Commissariat à l'Energie Atomique et aux Energies Alternatives and CNRS. This is the fourth article in the Thematic Minireview Series on Metals in Biology 2012.

[1] To whom correspondence should be addressed. E-mail: juan.fontecilla@ibs.fr.

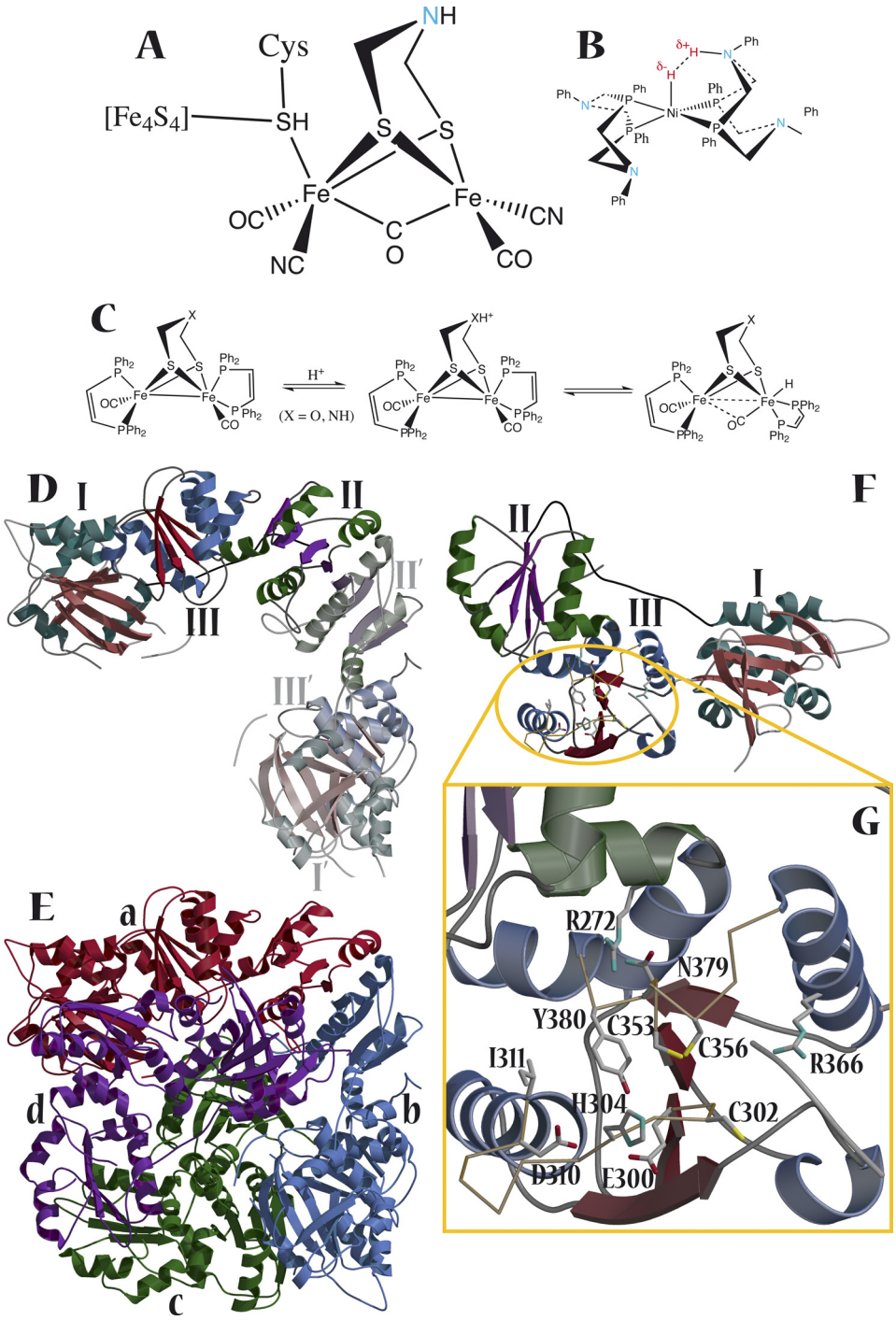

FIGURE 1. **[FeFe]-Hydrogenase active site, its bio-inspired models, and HydF, the scaffold where the active site is assembled.** *A*, the active site (H-cluster) of [FeFe]-hydrogenase depicted with nitrogen as the bridgehead atom (see text) (2). *B*, proposed intermediate state of a synthetic nickel complex for H_2 production with pendant amines (40, 41). *C*, functional model implying either an aza- or an oxadithiolate as the proton relay during catalysis by [FeFe]-hydrogenase (39). Although, in this model, both oxygen and nitrogen can be protonated at the bridgehead position of the dithiolate, only the latter would be physiologically relevant (39). *D*, crystal structure of dimeric apo-HydF from *T. neapolitana* (Protein Data Bank code 3QQ5) (21). The domains are numbered as in text: domain I is a GTPase, domain II is the domain of dimerization, and domain III is where the $[Fe_2]$ subcluster is assembled. *E*, tetrameric dimer of dimers. *F*, depiction of the region containing the conserved residues found near the three conserved cysteines. These could be part of the $[Fe_2]$ subcluster assembly site. *G*, magnification of the region shown in *F*.

have been recently characterized using several spectroscopic techniques (16, 19, 20). The EPR spectrum of non-reconstituted and reduced $HydF^{\Delta EG}$ displays signals that could be attributed to $[Fe_4S_4]^{1+}$ and $[Fe_2S_2]^{1+}$ clusters (16). Conversely, non-reconstituted reduced $HydF^{EG}$ exhibits only an $[Fe_4S_4]^{1+}$ cluster EPR signal (16, 19). When oxidized, another signal similar to that of the H-cluster is observed (16, 19). Contrary to what is observed when $HydF^{\Delta EG}$ is reconstituted, hyperfine sublevel correlation spectroscopy studies of $HydF^{EG}$ suggest that the fourth ligand of the $[Fe_4S_4]$ cluster is histidine (19). The authors proposed that this ligand bridges the $[Fe_4S_4]$ and $[Fe_2S_2]^{1+}$ clusters. The reconstituted $HydF^{\Delta EG}$ only displays a

signal corresponding to $[Fe_4S_4]^{1+}$, in agreement with a content of about four irons/protein monomer (14, 16). This observation suggests that the $[Fe_2S_2]$ cluster observed in the purified $HydF^{\Delta EG}$ cannot be reconstituted *in vitro*, requiring accessory proteins, which are also present in organisms that do not have an [FeFe]-hydrogenase. This may be due to the fact that this $[Fe_2S_2]$ cluster has to be coordinated by ligands other than cysteine. FTIR spectroscopy shows that, in its reduced state, $HydF^{EG}$ generates bands assigned to two CN^- and four terminal CO ligands (19). Upon oxidation, other bands appear, indicating that the sample contains species in different states (16, 19). Notably, a band at 1811 cm^{-1} reveals the presence of a bridging CO ligand. These results indicate that the center bound to HydF is similar to the $[Fe_2]$ component of the H-cluster. The same applies to EXAFS data, which show parameters similar to those observed for that cluster (20). The resemblance of the cluster assembled in HydF to the H-cluster is consistent with the observation that, when coexpressed with HydG and HydE, HydF displays significant hydrogen uptake activity (10).

The 3.0 Å resolution x-ray structure of the apo (GTP-free) form of HydF from *Thermotoga neapolitana* has been recently reported (21). As already suggested by its amino acid sequence, the protein is composed of three distinct structural domains (Fig. 1*D*). Domain I contains the GTP-binding pocket, and its fold is similar to that of other GTPases. Domain II is responsible for HydF dimerization. Domain III contains the three conserved cysteine residues responsible for the binding of the $[Fe_4S_4]$ cluster and is likely to harbor the scaffold site for the $[Fe_2]$ subcluster. Analysis of the crystal structure led the authors to conclude that HydF aggregates as a dimer of dimers (Fig. 1*E*), which is an inactive form of the protein. Indeed, in the tetramer, the putative scaffold site would not be accessible to the other Hyd proteins. HydF tetramers (or dimers of dimers) have been observed in solution in at least four different species, *T. neapolitana* and *Clostridium acetobutylicum* (21) and *Moorella thermoacetica* and *T. maritima*,[2] and they seem to be generally present *in vitro*. As indicated by modeling, the dimer of dimers is not compatible with GTP binding by domain I because of steric hindrance. By the same token, GTP binding might prevent tetramerization, allowing HydF to interact with its partners. Tetramerization might produce a resting state, which either stabilizes the protein or protects the solvent-exposed [FeS] cluster. Functional HydF is likely to be a dimer, exposing domains I and III to solvent, thus allowing for the interactions between partners that lead to the assembly of the $[Fe_2]$ subcluster. Intriguingly, domain III is topologically related to one subdomain of the H-domain of the HydA hydrogenase. However, as pointed out by Cendron *et al.* (21), the superposition of the two domains is rather poor at the loops and β-turns that define the cluster-binding pocket. This excludes the possibility of unambiguously identifying the $[Fe_2]$ subcluster-binding pocket, which could lead, in turn, to a model of the subcluster-loaded HydF. Nevertheless, it is noteworthy that the conserved Glu-300, His-304, Asp-310, Ile-311, Asn-379, and Tyr-380 residues are located close to the three invariant cysteine residues. Consequently, they could be part of the $[Fe_2]$ subcluster-binding pocket (Fig. 1, *F* and *G*). Potential iron ligands, such as glutamate and histidine, may be instrumental in the transition of an $[Fe_2S_2]$ rhomb to a fully assembled $[Fe_2]$ subcluster during the maturation process. Because $[Fe_4S_4]$ binding would require a rearrangement of the loop containing Cys-302, it appears that the amino acids that spatially define the subcluster-binding pocket in the active HydF do not adopt their correct conformations in the crystal structure. The structure of holo-HydF would be most useful in this respect.

HydG: A CO and CN^- Synthase—Amino acid sequence comparisons indicate that HydG should have the $(\beta\alpha)_8$ TIM barrel fold already found in biotin synthase (BioB) (22) and HydE (23) (see below). In addition, HydG proteins have an 80–90-residue-long C-terminal stretch (11). This region contains a conserved $CX_2CX_{22}C$ motif and is absolutely required for hydrogenase maturation (15). Preliminary characterization of HydG from *T. maritima* suggested the existence of an $[Fe_4S_4]$ cluster, in addition to the one typically found in radical *S*-adenosyl-L-methionine (SAM)[3] enzymes (24). This assumption has been confirmed by a recent characterization of *C. acetobutylicum* HydG after *in vitro* [FeS] cluster reconstitution (12). No fourth ligand for this cluster has been identified to date. Intriguingly, HydG expressed in *C. acetobutylicum* seems to harbor only one $[Fe_4S_4]$ cluster per monomer (19).

The amino acid sequence of the radical SAM domain of HydG resembles that of ThiH (11). The latter cleaves tyrosine, producing *p*-cresol and dehydroglycine (25). We have shown that HydG also cleaves tyrosine and produces *p*-cresol (Fig. 2, *A* and *C*) (11). This result is consistent with the 5-fold higher *in vitro* activation of an [FeFe]-hydrogenase by this aromatic amino acid (26). Shortly thereafter, it was demonstrated that HydG produces both CN^- and CO (12, 13). FTIR spectroscopic characterization of *in vitro* activated [FeFe]-hydrogenase in the presence of isotopically labeled tyrosine demonstrated that the CN^- and CO ligands originate from its -Cα-N and $-CO_2^-$ moieties, respectively (10).

Mutating two of the cysteine residues from the C-terminal stretch of the *C. acetobutylicum* HydG protein into serine does not impair CN^- production. Conversely, these mutations completely abolish CO synthesis, indicating that this process requires the second $[Fe_4S_4]$ cluster (Fig. 2, *A* and *C*) (27, 28). We concluded that, although CO and CN^- are produced at similar rates (12, 13), their syntheses are not simultaneous and are likely to occur at different locations of the protein (27, 28). A comparison of HydG and ThiH, using the HydE and BioB structures for amino acid sequence threading, indicates that the residues lining the TIM barrel cavity can be grouped into three layers (28): one layer common to all radical SAM enzymes involved in $[Fe_4S_4]$ binding and SAM cleavage, a second layer common to HydG and ThiH and probably involved in tyrosine binding, and a third layer containing residues that are different in ThiH and HydG (Fig. 2*C*). The latter reflects the dissimilar roles that the products resulting from tyrosine Cα–Cβ bond cleavage will play. Indeed, the dehydroglycine produced by

[2] L. Martin, Y. Nicolet, and J. C. Fontecilla-Camps, unpublished data.

[3] The abbreviations used are: SAM, *S*-adenosyl-L-methionine; DTN, dithiomethylamine.

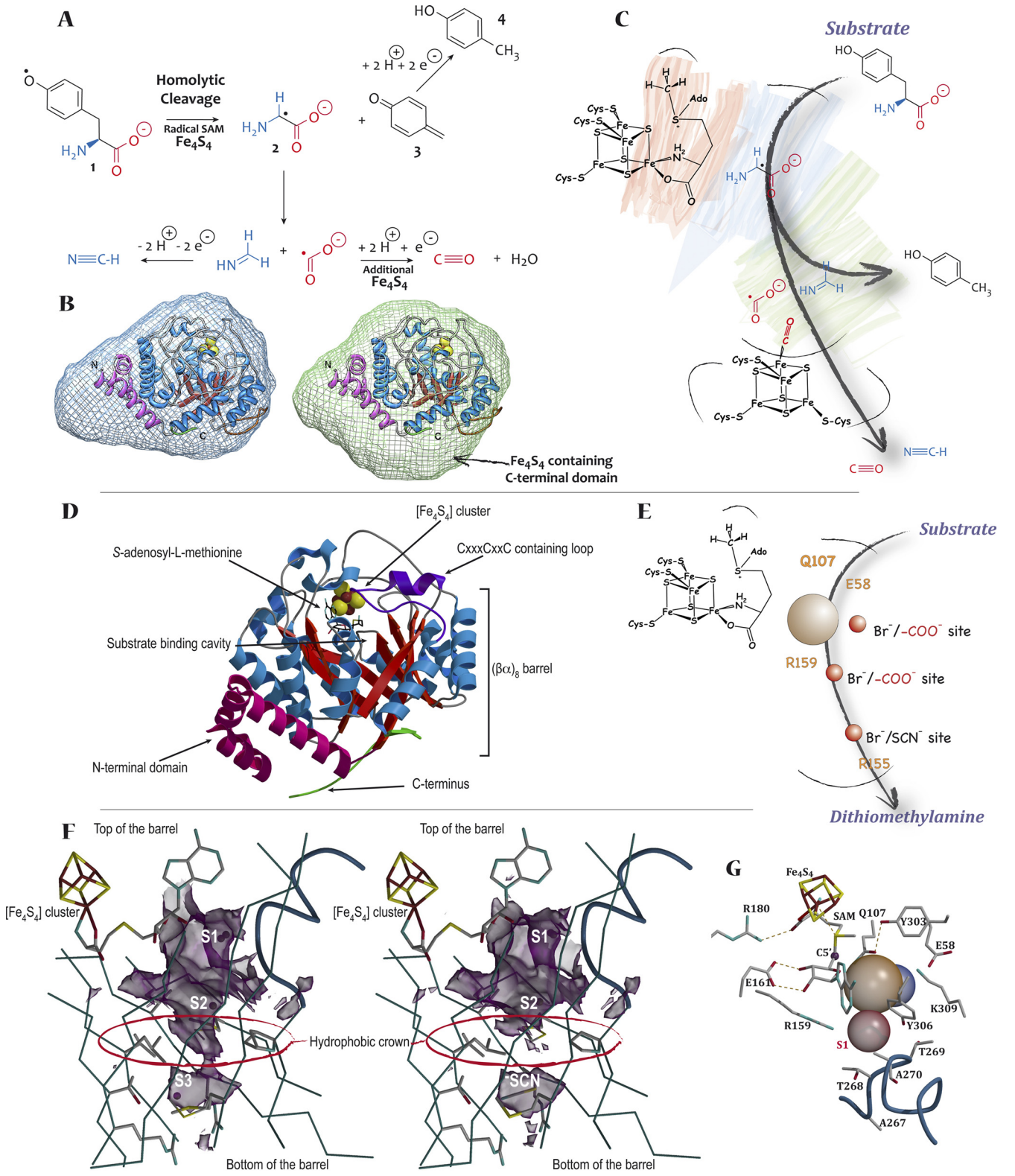

FIGURE 2. **Two radical SAM maturases HydG and HydE.** *A*, plausible reaction path for the generation of the CO and CN^- ligands of the [Fe_2] subcluster of [FeFe]-hydrogenase by HydG. *B*, small angle x-ray scattering-generated envelopes for C-terminally truncated HydG (*left*) and wild-type HydG (*right*) with a fitted model of the truncated form of the enzyme (28). Note the extra volume in the envelope of the latter that should correspond to the C-terminal [FeS] cluster-containing domain. *C*, depiction of the topology of the CO/CN^- synthesis by HydG from tyrosine (see text). *Shading* represent the SAM-binding region (*orange*), the substrate-binding region (*blue*), and the specificity region (*green*). See also Ref. 27. *D*, crystal structure of HydE from *T. maritima* (Protein Data Bank code 3CIW) (23). *E*, scheme of the internal cavity of HydE. The three anion-binding sites and residues known to be essential from mutagenesis studies are indicated. The *brown circle* depicts the substrate-binding region. The small organic active site ligand is assumed to be DTN (see text). *F*, effect of $^-$SCN binding (*right*) on the internal HydE cavity shape. The region where changes take place is indicated by a *red ellipse*. *G*, magnification of the HydE active site showing (i) the substrate-binding region (*large purple sphere*), anion-binding site S1 (*red sphere*), and a potential cation-binding site (*blue sphere*) and (ii) bound SAM with its 5′-carbon depicted as a *small brown sphere*. Conserved residues at the SAM- and substrate-binding sites known to play a role in HydE activity (23) are shown.

ThiH, rather than generating CO and CN^-, is subsequently inserted into thiamin in the vitamin B_1 synthetic pathway (25).

We have performed small angle x-ray scattering experiments using both wild-type HydG and a C-terminally truncated mutant. These studies show that the C-terminal stretch that coordinates the second $[Fe_4S_4]$ cluster forms a domain that interacts extensively with the bottom of the TIM barrel (Fig. 2*B*) (28). The truncation mutant is still capable of cleaving tyrosine to produce *p*-cresol (28). However, because of the detection limits of the techniques used to measure CN^- (13, 27), it is not clear whether small amounts of CN^- are still produced by the mutant (28).

On the basis of these results, we have proposed a mechanism that invokes reactions taking place along the internal cavity of HydG (Fig. 2*C*) (27, 28). It involves a glycyl radical resulting from cleavage of the Cα–Cβ bond of tyrosine. This radical would subsequently undergo deprotonation followed by homolytic decarboxylation, leading to the production of $H_2C{=}NH$ and a $^{\bullet}CO_2$ radical species. $H_2C{=}NH$ can be a precursor in HCN synthesis (Fig. 2*A*) (29). Conversely, $^{\bullet}CO_2$ can be reduced to CO through a metal-based reaction (30), which could occur at the available iron-binding site of the second $[Fe_4S_4]$ cluster (Fig. 2*C*). Further work will be required to elucidate the complete mechanism of CO and CN^- synthesis by HydG.

HydE: The Putative Small Dithiolate Ligand Synthase—As discussed above, HydG is responsible for CO and CN^- synthesis, and HydF serves as a scaffold for the $[Fe_2]$-containing subcluster assembly, prior to its insertion into the hydrogenase. Proceeding by elimination, HydE is most likely involved in the production of the small dithiolate $[Fe_2]$ ligand of the active site. The substrate of HydE is not known, but it must be a common metabolite because coexpressing the three maturases and the [FeFe]-hydrogenase in an organism lacking the latter, such as *E. coli*, leads to the production of active enzyme (8). As expected from previous multiple amino acid sequence alignments (31), the structure of HydE from *T. maritima* contains the $(\beta\alpha)_8$ TIM barrel and the $[Fe_4S_4]$ cluster responsible for SAM binding and cleavage already seen in BioB and typical of radical SAM proteins (23, 32). The structure confirms the presence of an additional site that also has three cysteine residues and binds an $[Fe_4S_4]$ cluster in solution (24). Despite numerous attempts to obtain an $[Fe_4S_4]$ cluster at this site in the HydE crystals, only an $[Fe_2S_2]$ cluster was observed in our structure. The significant similarity between HydE and BioB, which is responsible for sulfur atom insertion from an $[Fe_2S_2]$ cluster into dethiobiotin, suggested that the second cluster could be the sulfur source, involving a mechanism similar to that of BioB (33). However, the location of this cluster is different in the two proteins, and mutating the cysteine residues responsible for $[Fe_2S_2]$ cluster binding to HydE did not affect hydrogenase activity (23). This is consistent with the results of an amino acid sequence analysis of HydE from different organisms that unveiled two subclasses of enzyme, distinguishable by the presence or absence of the cysteine ligands to the second [FeS] cluster (23). This observation rules out this cluster as a possible sulfur source for biosynthesis of the small dithiolate $[Fe_2]$-bridging species. Three options for the origin of the sulfur atoms in this molecule may be considered. 1) HydE synthesizes it from a yet unknown substrate and an external sulfur source, such as an activated cysteine desulfurase; 2) the substrate of HydE already contains the required sulfur atoms; or 3) HydE synthesizes an intermediate, which reacts on the $[Fe_2S_2]$ cluster of HydF to produce the [FeFe]-dithiolate cluster directly at the scaffold site. No experimental evidence is available to discriminate between these three possibilities. However, it is worthwhile to mention that, under certain conditions, HydE co-purifies with HydF, suggesting a direct interaction between the two partners (9). In addition, in *C. reinhardtii*, *hydE* and *hydF* are fused as one gene (7).

The x-ray structure of HydE also reveals a large internal cavity, which spans the full length of the $(\beta\alpha)_8$ barrel (23). Its positive surface potential indicates that HydE should be able to bind molecules with negatively charged moieties. This was in fact confirmed by the presence of three distinct anion-binding sites in the structure (Fig. 2, *D–F*) (23). Moreover, an *in silico* docking experiment using 20,000 molecules, combined with site-directed mutagenesis experiments, allowed us to define a minimal substrate-binding volume close to SAM (Fig. 2*G*) (23). Some structural features required for binding to HydE near SAM could also be identified. Thus, the natural substrate should contain at least two negatively charged moieties, separated by enough atoms to allow their respective binding to sites S1 and S2, identified by bromide binding (Fig. 2, *E* and *F*) (23).

Crystal soaking experiments with several small molecules used as leads showed that thiocyanate binds HydE with high affinity at the third anion-binding site, S3, located at the bottom of the barrel (23). Although the 1.35 Å resolution x-ray structure has not provided further clues regarding the nature of the HydE substrate, ligand binding studies have been informative concerning the synthesis and transfer of the product of the enzyme to its partner. For instance, thiocyanate binding causes the rearrangement of a ring of conserved hydrophobic residues, dividing the internal cavity of HydE into two pockets (Fig. 2*F*) (23). Site-directed mutagenesis has shown that conserved residues, essential to HydE function, are present in both of these pockets (Fig. 2*G*) (23). This suggests that, after the radical-based reaction occurs at the substrate-binding pocket, the product will migrate to the bottom of the barrel, where thiocyanate binds, to be subsequently transferred to HydF (34). Thus, the ring of conserved hydrophobic residues may serve as a structural intermediate, exchanging information on the substrate/product binding status between pockets. It may also serve as a one-way valve to drive transfer of the small dithiolate species or its precursor to HydF. Both HydE and HydG may be described as nanofactories using their large internal cavities as assembly lines. Radical-based reactions are initiated at the top end near SAM, whereas intermediates and products move to the bottom end, where the latter are released.

Nature of the Bridgehead Atom of the Dithiolate-containing Small Active Site Molecule

In an initial report, Peters *et al.* (5) modeled the $[Fe_2]$ subcluster of the active site in *Clostridium pasteurianum* [FeFe]-hydrogenase I with two sulfide ions and a bridging water molecule, although it was stated that there was residual unexplained electron density. Subsequently, we reported the 1.5 Å

TABLE 1
Specific hydrogenase activities of purified enzymes and cell extracts

Organism	Hydrogenase activities of purified enzymes		Ref.
	Uptake	Evolution	
	$\mu mol\ H_2\ min^{-1}\ mg^{-1}$		
T. maritima	45–70	9–15	50
D. desulfuricans	19,300 (60,000)[a]	8,200	51
C. pasteurianum	5,500		52
T. vaginalis	662		53
Megasphaera elsdenii	9,000	7,000	54
C. reinhardtii		935	55
C. reinhardtii[b]		150	15
Clostridium thermoaceticum CODH		0.59	56
C. thermoaceticum PFOR[c]		0.14	56
Nickel rubredoxin		1.3×10^{-3}	54

Organism	Hydrogenase activities of cell extracts		Ref.
	Uptake	Evolution	
	$\mu mol\ H_2\ min^{-1}\ mg^{-1}$		
T. vaginalis		0.17/0.48	48 and 57
C. reinhardtii[d]		0.11	15
E. histolytica[e]		0.036	48
E histolytica[f]		0.0035	48
E. coli[d]		0.00035	15

[a] Activity after reductive activation.
[b] Coexpressed in *E. coli* with *C. acetobutylicum* maturases.
[c] PFOR, pyruvate:ferredoxin oxidoreductase.
[d] Activity per milliliter instead of per milligram of cell extract
[e] Expressed in *E. coli*.
[f] Overexpressed in *E. histolytica*.

resolution crystal structure of the enzyme from *Desulfovibrio desulfuricans* and showed that the two iron-bridging sulfur atoms are connected by three light atoms (4). At the usual resolutions, protein crystallography cannot distinguish between carbon, nitrogen, and oxygen, and at the time, we described that molecule as propane dithiolate. However, both structural and functional arguments led us later to conclude that the bridgehead atom should be nitrogen and the small molecule a dithiomethylamine (DTN) (6). First, in our structure, the bridgehead atom is 3.1 Å from the Sγ of Cys-178; this distance is compatible with an H-bond between the two atoms, as required for the proton transfer path proposed by Cornish *et al.* (36). Second, the heterolytic cleavage of H_2 requires both proton- and hydride-binding species. The bridgehead atom is ideally placed to play the role of a base so that the H_2 molecule gets polarized between this atom and the distal iron ion. This observation also favors nitrogen as the bridgehead atom because neither carbon nor oxygen could play that role under physiological conditions. The first step in proton transfer from the active site would then be the translocation of a proton bound to nitrogen through a facile Walden-like inversion.

Indirect spectroscopic and chemical evidence also favors nitrogen as the bridgehead atom. Using hyperfine sublevel correlation spectroscopy, Lubitz and co-workers (37) identified three distinct types of nitrogen atom (amine, cyanide, and ϵ-amino from lysine) at or in the vicinity of the *D. desulfuricans* [FeFe]-hydrogenase H-cluster. The detection of an amine at or near the active site of the enzyme provides strong evidence for nitrogen being the bridgehead atom of the bridging dithiolate. Furthermore, in a more recent publication, these authors showed that an H-cluster-mimetic small molecule containing a central nitrogen atom displays hyperfine couplings that are quite similar to those found in the H_{ox} state of the hydrogenase (38). The same situation applies when the respective ^{14}N nuclear quadrupole couplings are compared. Both studies have been complemented with theoretical analyses.

Rauchfuss and co-workers (39) compared functional models of the [FeFe]-hydrogenases containing carbon, oxygen, and nitrogen at the bridgehead position (Fig. 1*C*) and found that both azadithiolates and oxodithiolates can relay a proton to iron. However, only the former enables hydride formation from weak acids, which is relevant to biological catalysis that normally takes place at low overpotentials. DuBois and co-workers (40) provided what is perhaps the most impressive confirmation of the role of amines in hydrogen catalysis by small synthetic metal-containing catalysts. One of their catalysts can readily convert to a transition state (Fig. 1*B*), containing a hydride on a nickel ion and a proton on a pendant amine (41).

An alternative proposition for the identity of the bridgehead atom has been put forward by Szilagyi and co-workers (42). Using the 1.39 Å resolution structure of *C. pasteurianum* hydrogenase I and energy considerations, these authors concluded that the most likely bridgehead atom is oxygen (42). Conversely, in a more recent publication, Grigoropoulos and Szilagyi (43) proposed that the most favored biosynthetic pathway for the dithiolate ligand would start with a long alkyl chain and lead to propane dithiolate. The synthesis of this molecule would involve radical chemistry on an $[Fe_2S_2]$ cluster. As discussed above, the most likely candidate to catalyze the synthesis of the dithiolate ligand is HydE. Because the second [FeS] cluster of this enzyme is not conserved, the proposed mechanism would require migration of a radical species generated in HydE to, presumably, HydF.

In summary, although oxygen and carbon have also been proposed as the bridgehead atom of the small dithiolate species and a direct demonstration of its nature is lacking, accumulated spectroscopic and chemical evidence favors nitrogen in DTN. The identification of the substrate of HydE would settle this issue.

Maturation and Activity of [FeFe]-Hydrogenases without Maturases

Puzzling results have been obtained when expressing the structural hydrogenase genes in organisms devoid of the Hyd maturases and without the coexpression of these enzymes. Thus, the hydrogenase activity of lysates of *E. coli* transfected with the protozoan *Entamoeba histolytica* structural gene is ~10 times higher than the activity of the control *E. coli* lysate without it. (This information, along with the activities of other [FeFe]-hydrogenases not discussed here, is provided in Table 1.) In the same study, the hydrogenase activity of a non-transformed *Trichomonas vaginalis* extract was four to five times higher than that of *E. coli* lysates containing the recombinant *E. histolytica* hydrogenase (Table 1). In another report (44), extracts of the cyanobacterium *Synechocystis* sp. transfected with a *C. reinhardtii hydA* gene but without maturase genes displayed 5-fold higher hydrogenase activity than the non-transfected extracts (Table 1). However, the expression levels of active enzyme were very low (44).

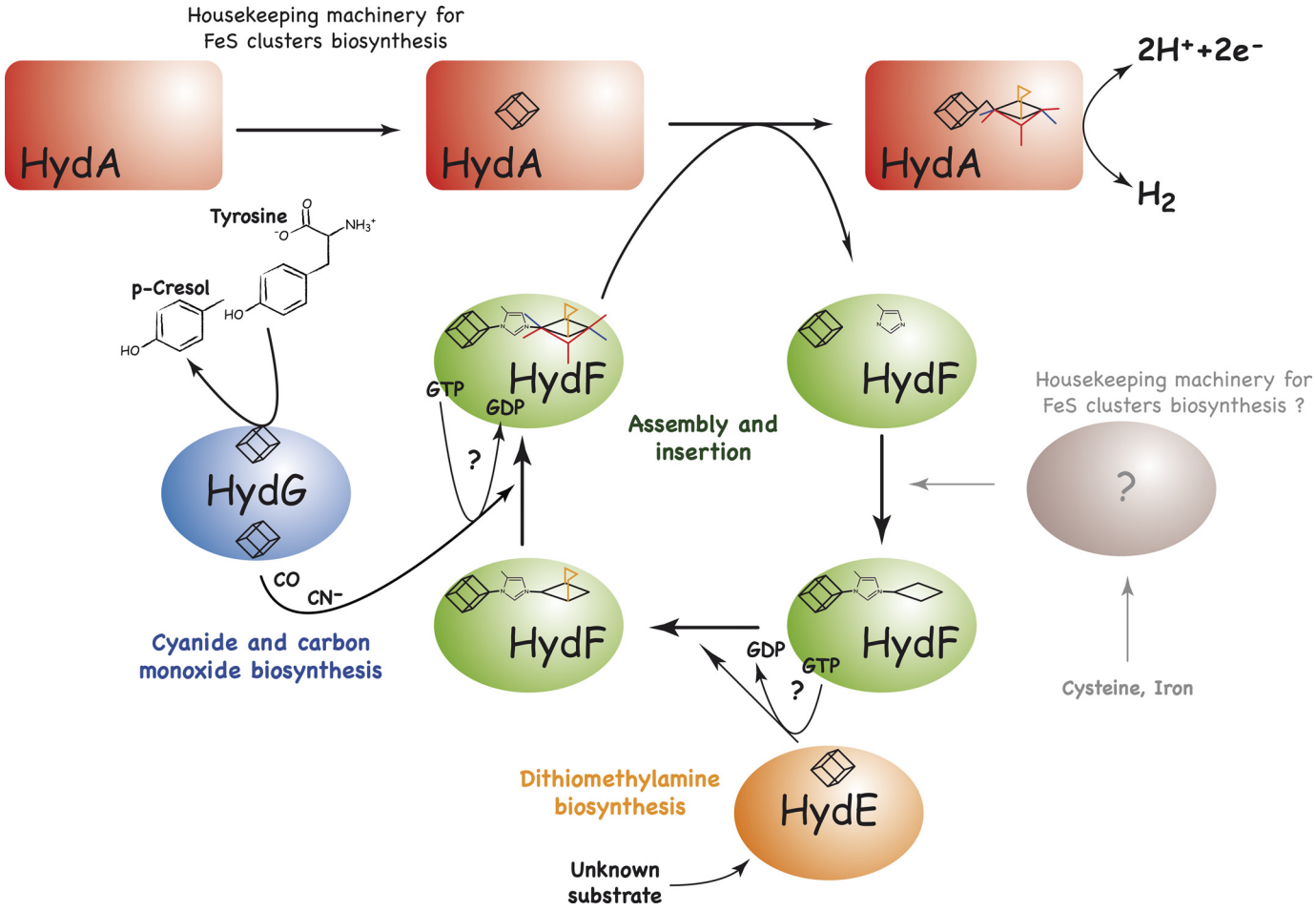

FIGURE 3. **Our working hypothesis concerning the assembly and insertion of the active site of [FeFe]-hydrogenases.** The scaffold protein HydF is the central component of the Hyd synthetic machinery. We favor a sequence in which HydE delivers its product to the scaffold before HydG because HydE and HydF interact very closely (8), and *hydE* and *hydF* are fused as one gene in *C. reinhardtii* (7). The purified $HydF^{\Delta EG}$ protein contains $[Fe_4S_4]$ and $[Fe_2S_2]$ clusters, probably bridged by a histidine residue (19). By the action of HydE, the $[Fe_2S_2]$ cluster either is replaced or is a substrate for the synthesis of an Fe_2DTN species. HydG subsequently donates the CN^- and CO ligands to the nascent [FeFe] subcluster. These two processes may require GTP hydrolysis. At this point, the species assembled in HydF to be transferred to HydA is similar to its active site and displays hydrogenase activity (20). After transferring its product to HydA, HydF should contain only an $[Fe_4S_4]$ cluster as the protein obtained after *in vitro* reconstitution (9). An external and yet unidentified protein may be required to reassemble the $[Fe_2S_2]$ cluster in HydF to start a new synthetic cycle. Here, we have assumed that its sulfide ions are originally generated from cysteine by a desulfurase (18).

The hydrogenase activity from cell extracts transfected with structural genes but without maturases remains very modest. Ideally, the specific activity of purified enzymes should be determined to be able to establish meaningful comparisons between, for instance, *E. histolytica* [FeFe]-hydrogenase and its very active bacterial counterparts (Table 1). Given the structural complexity of the hydrogenase active site (Fig. 1*A*), it seems very unlikely that it could be fully assembled without the HydE-G maturases. An alternative option could be a partially assembled active site, like the one observed in the crystal structure of *C. reinhardtii* hydrogenase, expressed in the absence of the corresponding maturases (45). Such a site that contains the $[Fe_4S_4]$ component of the H-cluster might still catalyze H_2 evolution, albeit at significantly lower levels than a correctly assembled active center. Low levels of hydrogen evolution have been detected in CO dehydrogenase and pyruvate:ferredoxin oxidoreductase in the presence of their substrates (Table 1), and nitrogenase naturally evolves H_2 during nitrogen fixation (1). These three enzymes have iron- and sulfur-containing clusters. Even a nickel-substituted rubredoxin displays some (very low) hydrogen evolution activity (Table 1).

The most intriguing case is the human pathogen *Giardia intestinalis*, which seems to lack both hydrogenosomes and hydrogenase maturase genes (46); it still has the structural hydrogenase gene, and it is reported to have detectable intrinsic hydrogen-evolving activity in its cytoplasm (47, 48). This activity (2 nmol/min/10^7 cells) is ~10 times lower than hydrogen evolution in *T. vaginalis* under the same conditions.

The low hydrogenase activity of protozoa in general seems to result from limited enzyme expression. As discussed above, it may also be related, in some cases, to partial assembly of the H-cluster due to the absence of maturases, essential for the synthesis of CO, CN^-, and the small dithiolate $[Fe_2]$-bridging molecule. Alternatively, in the latter cases, these gene products could have functions other than hydrogen evolution, this activity being vestigial. Indeed, *G. intestinalis* has been described as a recent derivative of an aerobic lineage (47), in which case, the hydrogenase gene would have been acquired by horizontal gene

transfer. Proteins like Narf and Nar may represent an extreme case of functional evolutionary divergence from [FeFe]-hydrogenase (49).

Conclusions

In this minireview, we have addressed the assembly process and the nature of the small dithiolate species of [FeFe]-hydrogenases. Because of the joint efforts of several laboratories, an increasingly clearer picture of the maturation process is emerging (Fig. 3). A major next step will be the identification of the substrate of HydE, which most likely is responsible for the synthesis of the small dithiolate-containing molecule at the active site. This will, in turn, definitively establish the identity of the bridgehead atom of the dithiolate. Another point that needs to be studied is the composition of the active site of hydrogenases found in organisms that lack the corresponding maturases. Given the complexity of the maturation process and the active site components, it would be very surprising to find a fully assembled H-cluster in the absence of the Hyd proteins.

REFERENCES

1. Rubio, L. M., and Ludden, P. W. (2005) Maturation of nitrogenase: a biochemical puzzle. *J. Bacteriol.* **187,** 405–414
2. Fontecilla-Camps, J. C., Volbeda, A., Cavazza, C., and Nicolet, Y. (2007) Structure/function relationships of [NiFe]- and [FeFe]-hydrogenases. *Chem. Rev.* **107,** 4273–4303
3. Shima, S., Pilak, O., Vogt, S., Schick, M., Stagni, M. S., Meyer-Klaucke, W., Warkentin, E., Thauer, R. K., and Ermler, U. (2008) The crystal structure of [Fe]-hydrogenase reveals the geometry of the active site. *Science* **321,** 572–575
4. Nicolet, Y., Piras, C., Legrand, P., Hatchikian, C. E., and Fontecilla-Camps, J. C. (1999) *Desulfovibrio desulfuricans* iron hydrogenase: the structure shows unusual coordination to an active site Fe binuclear center. *Structure* **7,** 13–23
5. Peters, J. W., Lanzilotta, W. N., Lemon, B. J., and Seefeldt, L. C. (1998) X-ray crystal structure of the Fe-only hydrogenase (CpI) from *Clostridium pasteurianum* to 1.8 angstrom resolution. *Science* **282,** 1853–1858
6. Nicolet, Y., de Lacey, A. L., Vernède, X., Fernandez, V. M., Hatchikian, E. C., and Fontecilla-Camps, J. C. (2001) Crystallographic and FTIR spectroscopic evidence of changes in Fe coordination upon reduction of the active site of the Fe-only hydrogenase from *Desulfovibrio desulfuricans*. *J. Am. Chem. Soc.* **123,** 1596–1601
7. Posewitz, M. C., King, P. W., Smolinski, S. L., Zhang, L., Seibert, M., and Ghirardi, M. L. (2004) Discovery of two novel radical *S*-adenosylmethionine proteins required for the assembly of an active [Fe]-hydrogenase. *J. Biol. Chem.* **279,** 25711–25720
8. McGlynn, S. E., Ruebush, S. S., Naumov, A., Nagy, L. E., Dubini, A., King, P. W., Broderick, J. B., Posewitz, M. C., and Peters, J. W. (2007) *In vitro* activation of [FeFe]-hydrogenase: new insights into hydrogenase maturation. *J. Biol. Inorg. Chem.* **12,** 443–447
9. McGlynn, S. E., Shepard, E. M., Winslow, M. A., Naumov, A. V., Duschene, K. S., Posewitz, M. C., Broderick, W. E., Broderick, J. B., and Peters, J. W. (2008) HydF as a scaffold protein in [FeFe]-hydrogenase H-cluster biosynthesis. *FEBS Lett.* **582,** 2183–2187
10. Kuchenreuther, J. M., George, S. J., Grady-Smith, C. S., Cramer, S. P., and Swartz, J. R. (2011) Cell-free H-cluster synthesis and [FeFe]-hydrogenase activation: all five CO and CN^- ligands derive from tyrosine. *PLoS ONE* **6,** e20346
11. Pilet, E., Nicolet, Y., Mathevon, C., Douki, T., Fontecilla-Camps, J. C., and Fontecave, M. (2009) The role of the maturase HydG in [FeFe]-hydrogenase active site synthesis and assembly. *FEBS Lett.* **583,** 506–511
12. Shepard, E. M., Duffus, B. R., George, S. J., McGlynn, S. E., Challand, M. R., Swanson, K. D., Roach, P. L., Cramer, S. P., Peters, J. W., and Broderick, J. B. (2010) [FeFe]-Hydrogenase maturation: HydG-catalyzed synthesis of carbon monoxide. *J. Am. Chem. Soc.* **132,** 9247–9249
13. Driesener, R. C., Challand, M. R., McGlynn, S. E., Shepard, E. M., Boyd, E. S., Broderick, J. B., Peters, J. W., and Roach, P. L. (2010) [FeFe]-Hydrogenase cyanide ligands derived from *S*-adenosylmethionine-dependent cleavage of tyrosine. *Angew. Chem. Int. Ed. Engl.* **49,** 1687–1690
14. Brazzolotto, X., Rubach, J. K., Gaillard, J., Gambarelli, S., Atta, M., and Fontecave, M. (2006) The [Fe-Fe]-hydrogenase maturation protein HydF from *Thermotoga maritima* is a GTPase with an iron-sulfur cluster. *J. Biol. Chem.* **281,** 769–774
15. King, P. W., Posewitz, M. C., Ghirardi, M. L., and Seibert, M. (2006) Functional studies of [FeFe]-hydrogenase maturation in an *Escherichia coli* biosynthetic system. *J. Bacteriol.* **188,** 2163–2172
16. Shepard, E. M., McGlynn, S. E., Bueling, A. L., Grady-Smith, C. S., George, S. J., Winslow, M. A., Cramer, S. P., Peters, J. W., and Broderick, J. B. (2010) Synthesis of the 2Fe subcluster of the [FeFe]-hydrogenase H-cluster on the HydF scaffold. *Proc. Natl. Acad. Sci. U.S.A.* **107,** 10448–10453
17. Mulder, D. W., Ortillo, D. O., Gardenghi, D. J., Naumov, A. V., Ruebush, S. S., Szilagyi, R. K., Huynh, B., Broderick, J. B., and Peters, J. W. (2009) Activation of $HydA^{\Delta EFG}$ requires a preformed [4Fe-4S] cluster. *Biochemistry* **48,** 6240–6248
18. Raulfs, E. C., O'Carroll, I. P., Dos Santos, P. C., Unciuleac, M. C., and Dean, D. R. (2008) *In vivo* iron-sulfur cluster formation. *Proc. Natl. Acad. Sci. U.S.A.* **105,** 8591–8596
19. Czech, I., Silakov, A., Lubitz, W., and Happe, T. (2010) The [FeFe]-hydrogenase maturase HydF from *Clostridium acetobutylicum* contains a CO and CN^- ligated iron cofactor. *FEBS Lett.* **584,** 638–642
20. Czech, I., Stripp, S., Sanganas, O., Leidel, N., Happe, T., and Haumann, M. (2011) The [FeFe]-hydrogenase maturation protein HydF contains an H-cluster-like [4Fe4S]-2Fe site. *FEBS Lett.* **585,** 225–230
21. Cendron, L., Berto, P., D'Adamo, S., Vallese, F., Govoni, C., Posewitz, M. C., Giacometti, G. M., Costantini, P., and Zanotti, G. (2011) Crystal structure of HydF scaffold protein provides insights into [FeFe]-hydrogenase maturation. *J. Biol. Chem.* **286,** 43944–43950
22. Berkovitch, F., Nicolet, Y., Wan, J. T., Jarrett, J. T., and Drennan, C. L. (2004) Crystal structure of biotin synthase, an *S*-adenosylmethionine-dependent radical enzyme. *Science* **303,** 76–79
23. Nicolet, Y., Rubach, J. K., Posewitz, M. C., Amara, P., Mathevon, C., Atta, M., Fontecave, M., and Fontecilla-Camps, J. C. (2008) X-ray structure of the [FeFe]-hydrogenase maturase HydE from *Thermotoga maritima*. *J. Biol. Chem.* **283,** 18861–18872
24. Rubach, J. K., Brazzolotto, X., Gaillard, J., and Fontecave, M. (2005) Biochemical characterization of the HydE and HydG iron-only hydrogenase maturation enzymes from *Thermotoga maritima*. *FEBS Lett.* **579,** 5055–5060
25. Kriek, M., Martins, F., Challand, M. R., Croft, A., and Roach, P. L. (2007) Thiamin biosynthesis in *Escherichia coli*: identification of the intermediate and by-product derived from tyrosine. *Angew. Chem. Int. Ed. Engl.* **46,** 9223–9226
26. Kuchenreuther, J. M., Stapleton, J. A., and Swartz, J. R. (2009) Tyrosine, cysteine, and *S*-adenosylmethionine stimulate *in vitro* [FeFe]-hydrogenase activation. *PLoS ONE* **4,** e7565
27. Nicolet, Y., Martin, L., Tron, C., and Fontecilla-Camps, J. C. (2010) A glycyl free radical as the precursor in the synthesis of carbon monoxide and cyanide by the [FeFe]-hydrogenase maturase HydG. *FEBS Lett.* **584,** 4197–4202
28. Tron, C., Cherrier, M. V., Amara, P., Martin, L., Fauth, F., Fraga, E., Correard, M., Fontecave, M., Nicolet, Y., and Fontecilla-Camps, J. C. (2011) Further characterization of the [FeFe]-hydrogenase maturase HydG. *Eur. J. Inorg. Chem.* **2011,** 1121–1127
29. Johnson, W. R., and Kang, J. C. (1971) Mechanisms of hydrogen cyanide formation from the pyrolysis of amino acids and related compounds. *J. Org. Chem.* **36,** 189–192
30. Grodkowski, J., and Neta, P. (2001) Copper-catalyzed radiolytic reduction of CO_2 to CO in aqueous solutions. *J. Phys. Chem. B* **105,** 4967–4972
31. Nicolet, Y., and Drennan, C. L. (2004) AdoMet radical proteins–from structure to evolution–alignment of divergent protein sequences reveals strong secondary structure element conservation. *Nucleic Acids Res.* **32,** 4015–4025

32. Frey, P. A., Hegeman, A. D., and Ruzicka, F. J. (2008) The radical SAM superfamily. *Crit. Rev. Biochem. Mol. Biol.* **43,** 63–88
33. Jarrett, J. T. (2005) The novel structure and chemistry of iron-sulfur clusters in the adenosylmethionine-dependent radical enzyme biotin synthase. *Arch. Biochem. Biophys.* **433,** 312–321
34. Nicolet, Y., Fontecilla-Camps, J. C., and Fontecave, M. (2010) Maturation of [FeFe]-hydrogenases: structures and mechanisms. *Int. J. Hydrogen Energy* **35,** 10750–10760
35. Deleted in proof
36. Cornish, A. J., Gärtner, K., Yang, H., Peters, J. W., and Hegg, E. L. (2011) Mechanism of proton transfer in [FeFe]-hydrogenase from *Clostridium pasteurianum*. *J. Biol. Chem.* **286,** 38341–38347
37. Silakov, A., Wenk, B., Reijerse, E., and Lubitz, W. (2009) ^{14}N HYSCORE investigation of the H-cluster of [FeFe]-hydrogenase: evidence for a nitrogen in the dithiol bridge. *Phys. Chem. Chem. Phys.* **11,** 6592–6599
38. Erdem, O. F., Schwartz, L., Stein, M., Silakov, A., Kaur-Ghumaan, S., Huang, P., Ott, S., Reijerse, E. J., and Lubitz, W. (2011) A model of the [FeFe]-hydrogenase active site with a biologically relevant azadithiolate bridge: a spectroscopic and theoretical investigation. *Angew. Chem. Int. Ed. Engl.* **50,** 1439–1443
39. Barton, B. E., Olsen, M. T., and Rauchfuss, T. B. (2008) Aza- and oxadithiolates are probable proton relays in functional models for the [FeFe]-hydrogenases. *J. Am. Chem. Soc.* **130,** 16834–16835
40. O'Hagan, M., Shaw, W. J., Raugei, S., Chen, S., Yang, J. Y., Kilgore, U. J., DuBois, D. L., and Bullock, R. M. (2011) Moving protons with pendant amines: proton mobility in a nickel catalyst for oxidation of hydrogen. *J. Am. Chem. Soc.* **133,** 14301–14312
41. Helm, M. L., Stewart, M. P., Bullock, R. M., DuBois, M. R., and DuBois, D. L. (2011) A synthetic nickel electrocatalyst with a turnover frequency above 100,000 s^{-1} for H_2 production. *Science* **333,** 863–866
42. Pandey, A. S., Harris, T. V., Giles, L. J., Peters, J. W., and Szilagyi, R. K. (2008) Dithiomethylether as a ligand in the hydrogenase H-cluster. *J. Am. Chem. Soc.* **130,** 4533–4540
43. Grigoropoulos, A., and Szilagyi, R. K. (2010) Evaluation of biosynthetic pathways for the unique dithiolate ligand of the [FeFe]-hydrogenase H-cluster. *J. Biol. Inorg. Chem.* **15,** 1177–1182
44. Berto, P., D'Adamo, S., Bergantino, E., Vallese, F., Giacometti, G. M., and Costantini, P. (2011) The cyanobacterium *Synechocystis* sp. PCC 6803 is able to express an active [FeFe]-hydrogenase without additional maturation proteins. *Biochem. Biophys. Res. Commun.* **405,** 678–683
45. Mulder, D. W., Boyd, E. S., Sarma, R., Lange, R. K., Endrizzi, J. A., Broderick, J. B., and Peters, J. W. (2010) Stepwise [FeFe]-hydrogenase H-cluster assembly revealed in the structure of HydA$^{\Delta EFG}$. *Nature* **465,** 248–251
46. Pütz, S., Dolezal, P., Gelius-Dietrich, G., Bohacova, L., Tachezy, J., and Henze, K. (2006) [Fe]-Hydrogenase maturases in the hydrogenosomes of *Trichomonas vaginalis*. *Eukaryot. Cell* **5,** 579–586
47. Lloyd, D., Ralphs, J. R., and Harris, J. C. (2002) *Giardia intestinalis*, a eukaryote without hydrogenosomes, produces hydrogen. *Microbiology* **148,** 727–733
48. Nixon, J. E., Field, J., McArthur, A. G., Sogin, M. L., Yarlett, N., Loftus, B. J., and Samuelson, J. (2003) Iron-dependent hydrogenases of *Entamoeba histolytica* and *Giardia lamblia*: activity of the recombinant entamoebic enzyme and evidence for lateral gene transfer. *Biol. Bull.* **204,** 1–9
49. Nicolet, Y., Cavazza, C., and Fontecilla-Camps, J. C. (2002) Fe-only hydrogenases: structure, function, and evolution. *J. Inorg. Biochem.* **91,** 1–8
50. Verhagen, M. F., O'Rourke, T., and Adams, M. W. (1999) The hyperthermophilic bacterium *Thermotoga maritima* contains an unusually complex iron hydrogenase: amino acid sequence analyses *versus* biochemical characterization. *Biochim. Biophys. Acta* **1412,** 212–229
51. Hatchikian, E. C., Forget, N., Fernandez, V. M., Williams, R., and Cammack, R. (1992) Further characterization of the [Fe]-hydrogenase from *Desulfovibrio desulfuricans* ATCC 7757. *Eur. J. Biochem.* **209,** 357–365
52. Adams, M. W. (1990) The structure and mechanism of iron hydrogenases. *Biochim. Biophys. Acta* **1020,** 115–145
53. Payne, M. J., Chapman, A., and Cammack, R. (1993) Evidence for an Fe-type hydrogenase in the parasitic protozoan *Trichomonas vaginalis*. *FEBS Lett.* **317,** 101–104
54. Saint-Martin, P., Lespinat, P. A., Fauque, G., Berlier, Y., Legall, J., Moura, I., Teixeira, M., Xavier, A. V., and Moura, J. J. (1988) Hydrogen production and deuterium-proton exchange reactions catalyzed by *Desulfovibrio* nickel(II)-substituted rubredoxins. *Proc. Natl. Acad. Sci. U.S.A.* **85,** 9378–9380
55. Happe, T., and Naber, J. D. (1993) Isolation, characterization, and N-terminal amino acid sequence of hydrogenase from the green alga *Chlamydomonas reinhardtii*. *Eur. J. Biochem.* **214,** 475–481
56. Menon, S., and Ragsdale, S. W. (1996) Unleashing hydrogenase activity in carbon monoxide dehydrogenase/acetyl-CoA synthase and pyruvate: ferredoxin oxidoreductase. *Biochemistry* **35,** 15814–15821
57. Ellis, J. E., Cole, D., and Lloyd, D. (1992) Influence of oxygen on the fermentative metabolism of metronidazole-sensitive and -resistant strains of *Trichomonas vaginalis*. *Mol. Biochem. Parasitol.* **56,** 79–88